S. Nikzad DDS, MSc[1]
A. Azari DDS, MSc[1]
F. Hossein Khezri DDS[2]

Diagnosis of a Lingual Mandibular Bone Defect (Stafne's Bone Defect) by CT Scan

The lingual mandibular bone defect, which is also known as Stafne's bone defect, is a rare entity commonly affecting the posterior lingual part of the mandible. Although this lesion usually contains normal connective tissue compartments, it may be misinterpreted as tumor like lesions. In this manuscript, based on the density analysis of the CT images and through use of a simplified quantification system, a novel approach has been introduced which attempts to differentiate the benign nature of the defect.

Keywords: Lingual Mandibular Bone Defect, Stafne's Defect, Computer Tomography, Dental Implants

Introduction

Stafne's bone defect, which is known as lingual mandibular cavity, was first described by Stafne in 1942.[1] This rare entity characterized as a round or ovoid radiolucency which was well defined and located below the inferior alveolar canal; most frequently shows between the first molar and the angle of the mandible. The defect is more prevalent among men and is usually found accidentally during the diagnostic phase.[2,3] It was believed that this entity is a developmental defect and may be produced by the inward pressures exerted by the salivary gland on bony surfaces of the mandible.[4,5] Although the defect was first reported to be in the lingual posterior regions of the mandible and were unilateral, bilateral lesions, lesions above the mandibular canal, lesions on the buccal side of the ascending ramus and even lesions in the anterior part of the mandible have also been reported.[6-10] The bony defect may contain salivary gland, connective tissue, fat, lymphoid tissue, muscle or blood vessels and sometimes empty cavities have also been reported.[4-12]

Due to the painless and symptom-free nature of the lesion, non-invasive methods such as CAT scanning have been suggested to analyze Stafne's defect. In fact, CT scan and MRI are the modalities of choice, which may assist clinicians to better differentiate this defect from more frequent mandibular radiolucencies such as traumatic bone cysts and ameloblastomas. The CT may also be used as both diagnostic and follow up imaging and this enables the clinician to spare the patient from discomfort of sialography or other invasive diagnostic methods. This paper intends to describe the confirmative role of qualitative CT and CT densitometry by colorful differentiation in the diagnosis of Stafne bone cyst without the need for histopathology.

1. Associate Professor, Department of Prosthodontics, Faculty of Dentistry, Tehran University of Medical Sciences, Tehran, Iran.
2. Postgraduate Student, Department of Prosthodontics, Faculty of Dentistry, Tehran University of Medical Sciences, Tehran, Iran.

Corresponding Author:
Abbas Azari
Address: Department of Prosthodontics, Faculty of Dentistry, Tehran University of Medical Sciences, Quds Street, Tehran, Iran.
Tel: +9821 6640 2095
Fax: +9821 2257 6968
E.mail: azari@sina.tums.ac.ir.

Received January 26, 2009;
Accepted after revision June 28, 2009.

Iran J Radiol 2010;7(1):27-30

Case Report

A 58-year-old man with progressive wear of both maxillary and mandibular teeth was referred to the department of prosthodontics, Dental Faculty, Tehran University of Medical Sciences. The patient's demands were treatment of dentition wearing and implant/prosthetic restoration of edentulous spaces. At first step, a plain panoramic radiograph was ordered as a prerequisite for starting the treatment. The preliminary analysis showed a well defined radiolucency which was located on the right side of the mandible just below the inferior alveolar canal near the gonial angle (Fig. 1).

The patient had no complaints referring to the mandible. Clinical examination revealed no asymmetry or lymphadenopathy. Medical history showed that the patient was under routine check-up for this radiolucency for over two years, but because of the constant size and symptom-free nature of the defect, no treatment had been prescribed or recommended by previous physicians. In order to avoid unnecessary exploration of this defect before the beginning of the treatment phase, a CT scan was requested to confirm the diagnosis of the entity.

CT examination was performed using GE Medical Systems/HiSpeed QX (General Electric, USA) operated at 100KV and 89.10 mAs. A planning line was drawn along the center of the mandibular jaw arch, bellow the root of the remaining teeth. Images were then reconstructed into orthoradial (slice thickness 0.6 mm) and panoramic views with a thickness of 1.25 mm. The algorithm used was Bone-Plus and the FOV was 17 cm. The acquisitioned images were then rendered to a dedicated software program (Simplant Pro™ Ver. 12, Materialise Dental, Lueven, Belgium). This software was preliminarily released for 3D evaluation of the patient's anatomy, virtually placed implant(s) and subsequently to place real implants by designing custom made surgical templates, which are used during surgical intervention. The powerful features of this software make it easy to segment, mask and optimize the CT images in a way that an average clinician can manipulate it with ease (Fig. 2).

The principles used are well described in the literature.[13,14]

Analyzing of axial images showed right mandibular lingual wall defect with thinning of the buccal cortical bone (Fig. 3).

Coronal and sagittal images confirmed lingual wall defect of the lesion (Fig. 4).

Fig. 1. Panoramic plain radiograph of a 58-year-old man with a well-defined radiolucent defect at the left side of the mandible at the first visit (arrows).

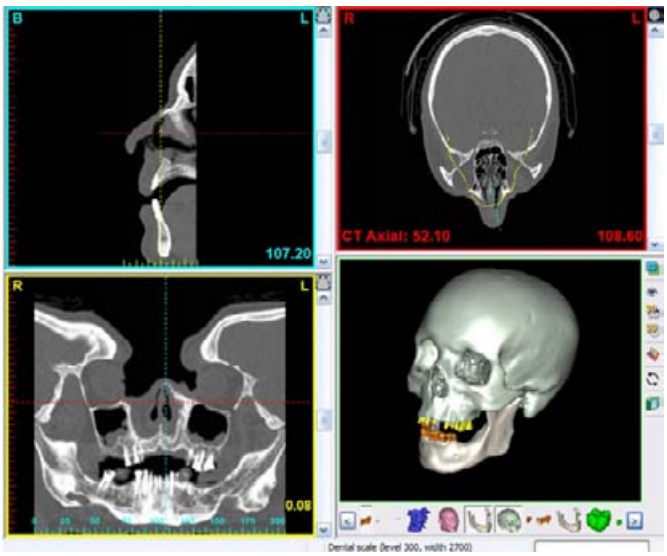

Fig. 2. A four panel view of software. Each plane was designed to show the patient's anatomy in every aspect. The 3D reconstructed model may be helpful during diagnosis and implant planning.

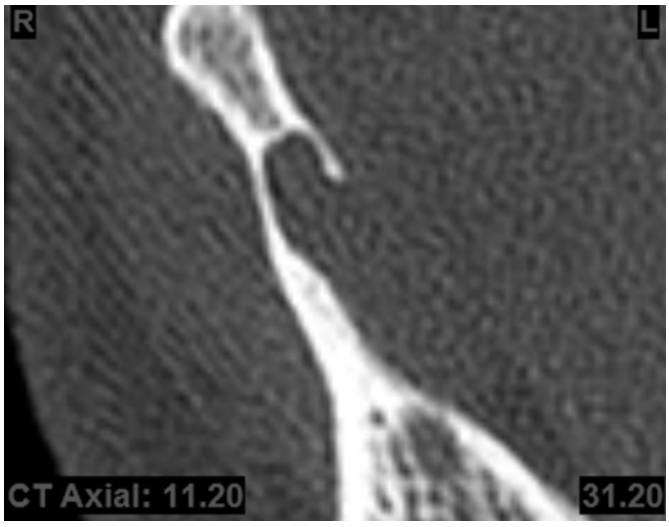

Fig. 3. Axial image of the defect.

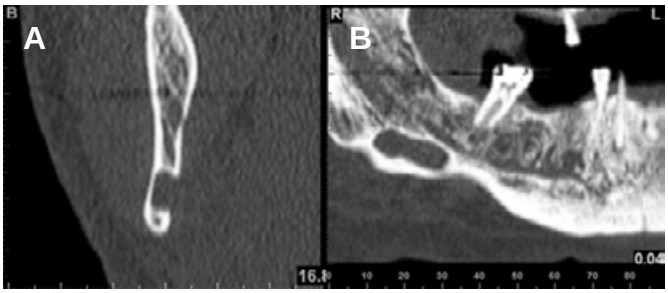

Fig. 4. Sagittal (**A**) and panoramic (**B**) view of the defect.

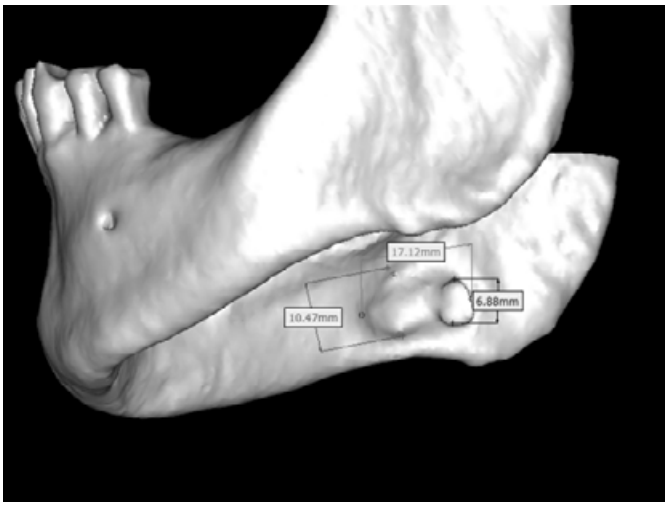

Fig. 5. 3D measurement of the defect on 3D model. This feature precisely determines the dimensions of the defect in actual 3D.

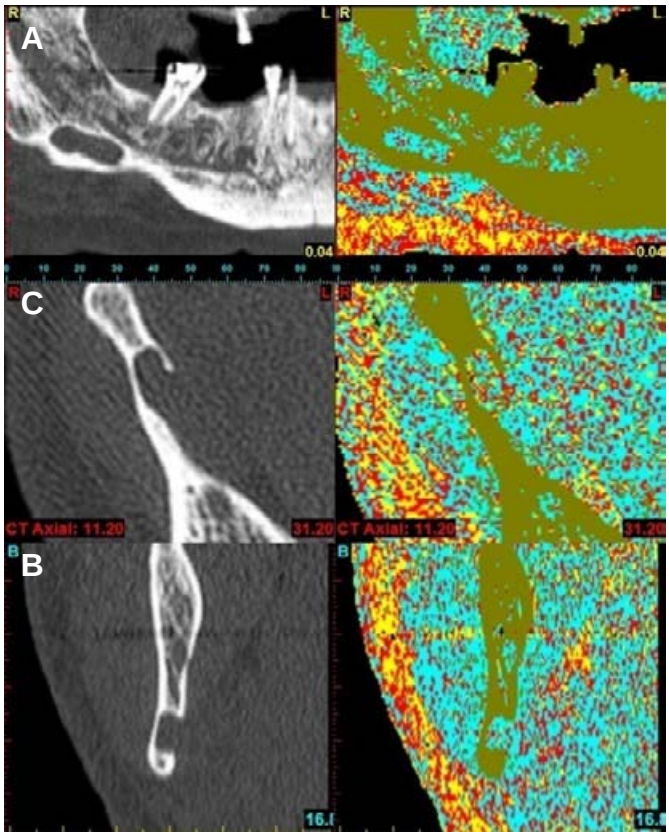

Fig. 6. Colorful segmentation and differentiation of the defect by means of CT density color scale. This color scale places four colors next to each other, representing the different types of tissue. The density scale is based on the relation between ranges of Hounsfield Units and the different tissue types which is demonstrated in panoramic (**A**), axial (**B**) and sagittal images (**C**).

3D reconstructed model of the object revealed two concavities, one ovoid and one round in shape, located at the right lingual side just bellow the mandibular canal and near the angle of the mandible. The dimensions of the defect were measured three dimensionally by software on the 3D model (Fig. 5).

For better evaluation, it was decided to use the ability of software to differentiate various parts of anatomy by color grouping of the Hounsfield Unit (HU). In this manner, we could separate each part of the proposed organ in colorful sketch rather than gray alone. To calibrate the software, four different ranges of CT density were defined by color as bellow:

From -300 to -101 HU (Yellow)
From -100 to -1 HU (Red)
From 0 to 150 HU (Blue)
Above 151 HU (Dark green)

The color differentiation shows that the main content of defect was in the range of glandular tissue (~40 HU, blue), but some areas for fat (≤-100 HU, yellow) and muscle (~50 HU, blue) can also be withdrawn. The CT density of defect is somewhat different from the muscles around the mandibular angle (Fig. 6).

Discussion

Diagnosis of Stafne's bone defect is necessary in order to avoid invasive treatments such as bone exploration and trephination. 3D radiographs like CT are able to determine borders of the lesion and its 3D shape. The quantitative nature of CT and advanced analytical software makes it possible to truly determine the inner compartment of intra-osseous defects such as Stafne's cavity. There are some reports regarding the CT density of submandibular glands. According to these reports, the fat content of this tissue is less than the parotid glands and therefore, is closer to muscle density (approximately 40 HU).[15] The result of this simplified method on the demonstrated mandibular defect showed that the HU is in the range of submandibular tissue/muscle and the benign nature

of the intra-osseous cavity in the patient's mandible was distinguished. Based upon the results of this CT scan study, it may be assumed that the use of color grouping of HU was quite helpful to quickly individualize the content of defective area from adjacent tissues.

In conclusion, although diagnosing Stafne's defect based on plain radiography is possible, confirmatory 3D radiographs are often useful. In these cases, a CT scan can be more definitive. This valuable modality has a great aid from both diagnostic and follow-up points of view and this enables clinicians to spare patients from discomfort of surgery or sialography. The dedicated software programs like the one used in this study may help clinicians in the better diagnosis of the defect and prevent the unnecessary treatment. Based upon the sophisticated approach described in this paper, biopsy was not necessary and one can easily determine the content of intra-osseous defects by just looking on the areas, which are colonized by color grouping and segmentation. Further assessment of this method is suggested for other similar lesions.

References

1. Stafne EC. Bone cavities situated near the angle of mandible. J Am Dent Assoc 1942;29:1969-72.
2. Shimizu M, Osa N, Okamura K, Yoshiura K. CT analysis of the Stafne's bone defects of the mandible. Dentomaxillofac Radiol 2006 Mar;35(2):95-102.
3. Goٞmez CQ, Castellٞn EV, Aytés LB, Escoda CG. Stafne bone cavity: a retrospective study of 11 cases. Med Oral Patol Oral Cir Bucal 2006;11:277-80.
4. Nah KS, Jung YH, Cho BH. Unusual Stafne bone cavity mimicking infected cyst or neural origin tumor. Korean J Oral Maxillofac Radiol 2007;37:221-3.
5. Philipsen HP, Takata T, Reichart PA, Sato S, Suei Y. Lingual and buccal mandibular bone depressions: a review based on 583 cases from a world-wide literature survey, including 69 new cases from Japan. Dentomaxillofac Radiol 2002 Sep;31(5):281-290.
6. Katz J, Chaushu G, Rotstein I. Stafne's Bone cavity in the anterior mandible: a possible diagnostic challenge. J Endod 2001;27(4):304-7.
7. Lello GE, Makek M. Stafne's mandibular lingual cortical defect: Discussion of aetiology. J Maxillofac Surg 1985 Aug;13(4):172-6.
8. Choukas NC. Developmental submandibular gland defect of the mandible: review of the literature and report of two cases. J Oral Surg 1973 Mar;31(3):209-11.
9. Correll RW, Jensen JL, Rhyne RR. Lingual cortical mandibular defects: a radiographic incidence study. Oral Surg Oral Med Oral Pathol 1980 Sep;50(3):287-91.
10. Chen CY, Ohba T. An analysis of radiological findings of Stafne's idiopathic bone cavity. Dentomaxillofac Radiol 1981;10(1):18-23.
11. Reuter I. An unusual case of Stafne bone cavity with extra-osseous course of the mandibular neurovascular bundle. Dentomaxillofac Radiol 1998 May;27(3):189-91.
12. Segev Y, Puterman M, Bodner L. Stafne bone cavity-magnetic resonance imaging. Med Oral Patol Oral Cir Bucal 2006 Jul;11(4):345-7.
13. Nikzad S, Azari A. CT-derived planning and surgery for implant dentistry. Iranian J Radiol 2008;5(3):177-9.
14. Azari A, Nikzad S. Kabiri A. Using computer-guided implantology in flapless implant surgery of a maxilla: a clinical report. J Oral Rehabil 2008 Sep;35(9):690-4.
15. Bailey BJ, Johnson JT, Newlands SD. Head and Neck Surgery-Otolaryngology. 4th Ed. Philadelphia: Lippincott Williams & Winkins; 2001. p. 529.